Published by :
http://www.ijert.org

International Journal of Engineering Research & Technology (IJERT)
ISSN: 2278-0181
Vol. 8 Issue 09, September-2019

Inverse Band Reject and All Pass Filter Structure Employing CMOS CDBAs

Ram Bhagat
Department of Electrical Engineering
Delhi Technological university
Delhi, India

D. R. Bhaskar
Department of Electronics and Communication Engineering
Delhi Technological university
Delhi, India

Pragati Kumar
Department of Electrical Engineering
Delhi Technological university
Delhi, India

***Abstract*— In this paper a new voltage-mode (VM) circuit for the realization of second order tuneable inverse band reject filter (IBRF) and inverse all pass filter (IAPF) have been introduced. The proposed circuit uses two current differencing buffered amplifiers (CDBA), two capacitors and four/five resistors. PSPICE simulation results employing CMOS CDBA implemented in 0.18µm CMOS TSMC technology have been presented to validate the workability of the configuration.**

Keywords*— *Analog Inverse Filters, Current Differencing Buffered Amplifier, Analog Signal Processing

I. INTRODUCTION

An analog inverse filter provides frequency selective characteristics which are opposite to those of the corresponding analog filter. These inverse filters are used to remove the effect of distortion introduced in the signal while it is processed through a system. Inverse filters find applications in control, instrumentation and communication systems [1]. Recently, a number of analog inverse active filterswith different properties have been realised with different active building blocks(ABB) like operational amplifiers (op-amps) [2], current feedback operational amplifiers (CFOAs) [3]-[7], second generation current conveyors CCIIs [8], [9], four terminal floating nullors (FTFNs) [10], [11], operational transresistance amplifiers (OTRAs) [13], [14] current differencing buffered amplifiers (CDBAs) [15], [16], current differencing transconductance amplifiers CDTAs [17], [18], operational transconductance amplifiers OTAs [19], differential difference current conveyors (DDCCs) [20] and voltage differencing transconductance amplifiers (VDTAs) [21]. However, there are few number of research publications for realising second order IBRF [3], [4], [7], [12], [14], [16] and IAPF [11], [12] and [14].

The CDBA has received prominent attention in analog signal processing and signal generation circuits due to its important property of providing at its input terminals virtual ground, which eliminates the effect of parasitic at the input terminals. Apart from this, its low output impedance enables the CDBA based circuit configurations to be cascaded easily.

From existing literature survey, it has been observed that only two circuit structures have been reported so far to realize second-order inverse active filters employing CDBAs [15], [16]. [15] has reported two CDBA based second order inverse low pass filter (ILPF) with four resistors and two capacitrs, inverse high pass filters (IHPF) using two resistors and four capacitors and inverse band pass filter (IBPF) with three resistors and three capacitors whereas in [16] the ILPF circuit is realized with four resistors and two capacitors the other four circuits namely, IHPF, IBPF, IBRF and IAPF have been realised with 3-4 capacitors and 2-4 resistors. Also none of these two reported inverse filters have utilized the intrinsic (current differencing) property of the CDBA, as n-terminal of one of the CDBA has been left open resulting into employment of more than two capacitors for realization of second order inverse filters of different types in many cases (IBPF, IHPF, IBRF and IAPF).

Therefore, the purpose of this communication is to present a new inverse filter circuit configuration employing two CDBAs with their intrinsic (current differencing) property fully utilized, four/five resistors and only two capacitors along with a switch. The realised second order IBRF has independent control of cut-off frequency and bandwidth while IAPF has independent tunability of cut-off frequency. The workability of the presented inverse filters has been verified using PSPICE simulations implemented in TSMC 0.18µm CMOS technology.

II. THE PROPOSED CONFIGURATION

The symbolic representation of the CDBA is shown in Fig.1, where p and n are current input terminals (with ideally zero input impedances), w is the voltage output terminal (ideally zero output impedance) and z is the current output terminal (ideally infinite output impedance).

The characterising terminal equations of an ideal CDBA are given by:

$$I_z = (I_p - I_n),\ V_p = 0 = V_n \text{ and } V_w = V_z \qquad (1)$$

The proposed configuration for the realization of IBRF and IAPF with two capacitors and four/five resistors is shown in Fig. 2.

International Journal of Engineering Research & Technology (IJERT)
ISSN: 2278-0181
Vol. 8 Issue 09, September-2019

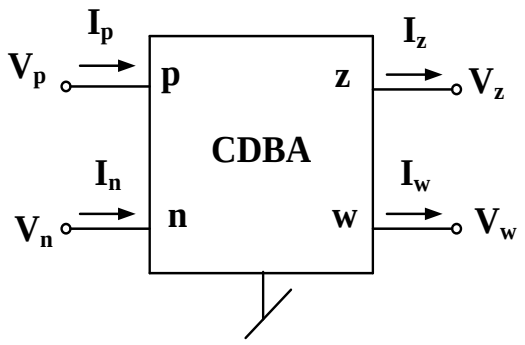

Fig. 1 Symbolic representation of CDBA

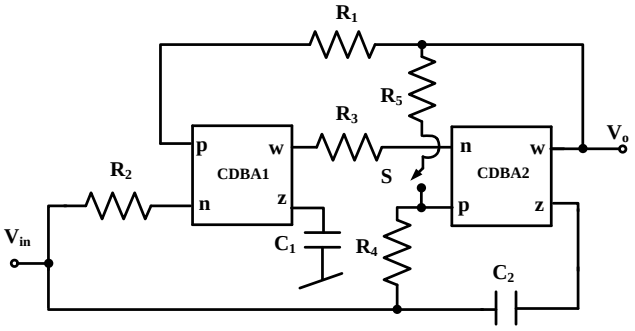

Fig. 2. The proposed inverse filer structure

Realization of IBRF and IAPF responses from Fig. 2 is as follows:

Case I: When switch 'S' is open the resulting transfer function becomes

$$\frac{V_o(s)}{V_{in}(s)} = \frac{1}{\dfrac{s^2 + \dfrac{1}{R_1R_3C_1C_2}}{s^2 + \dfrac{1}{R_4C_2}s + \dfrac{1}{R_2R_3C_1C_6}}} \quad (2)$$

which represents an IBRF with cut-off frequency (ω_0) and bandwidth (BW) given by:

$$\omega_o = \frac{1}{\sqrt{R_2R_3C_1C_2}} \quad \text{For} R_1 = R_2 \text{ and}$$
$$BW = \frac{1}{R_4C_2} \quad (3)$$

Case II: When switch 'S' is closed the resulting transfer function will be given by:

$$\frac{V_o(s)}{V_{in}(s)} = \frac{1}{\dfrac{s^2 - \dfrac{1}{R_7C_6}s + \dfrac{1}{R_1R_3C_1C_2}}{s^2 + \dfrac{1}{R_4C_2}s + \dfrac{1}{R_2R_3C_1C_2}}} \quad (4)$$

which realizes an IAPF with ω_0 and *BW* given by:

$$\omega_o = \frac{1}{\sqrt{R_2R_3C_1C_2}} \quad \text{For} R_1 = R_2 \text{ and}$$
$$BW = \frac{1}{R_4C_2} \text{For} R_4 = R_5 \quad (5)$$

Thus, it is clear that from equation (3), both ω_0 and *BW* can be tuned independently i.e. ω_0 through R_3/C_4 and *BW* through R_4

III. NON-IDEAL ANALYSIS

The non-ideal representation of the CDBA taking into account the parasitic at various terminals is shown in Fig.3, where parallel combination of R_z and $1/sC_z$ is the parasitic impedance at port z, R_p and R_n are the parasitic resistances at terminals p and n respectively and R_o is the parasitic output resistance at terminal w.

A practical CDBA can be described [22] by the following relationships that take into account the non-idealities of the device:

$$V_p = V_n = 0, I_Z = \beta_p I_P - \beta_n I_n \text{and} V_W = \alpha V_Z \quad (6)$$

where $\beta_P = (1-\varepsilon_P)$ and $\varepsilon_p(|\varepsilon_p| << 1)$ is the current tracking error from p-terminal to z-terminal, $\beta_n = (1-\varepsilon_n)$ where $\varepsilon_n(|\varepsilon_n| << 1)$ is the current tracking error from n-terminal to z-terminal, and $\alpha = (1-\varepsilon_v)$ with $\varepsilon_v(|\varepsilon_v| << 1)$ is the voltage tracking error from *z*-terminal to w-terminal of the CDBA. In addition to the above, if we also consider parasitic impedances at z-terminal and parasitic resistances at p, n and w terminals of CDBA as shown in Fig. 3 and reanalyze the circuits of Fig. 2, we get the following non-ideal transfer functions of inverse active filters:

The non-ideal expression of IBRF is given by

$$\left.\frac{V_o(s)}{V_{in}(s)}\right|_{IBRF} = \frac{1}{\dfrac{\dfrac{1}{\alpha_2}s^2 + Bs + C}{s^2 + Ms + N}} \quad (7)$$

where

$$B = \frac{1}{\alpha_2C_1(C_2 + C_{Z2}) + \alpha_2C_{Z1}(C_2 + C_{Z2})}\left(\frac{C_1}{R_{z2}} + \frac{C_{z1}}{R_{z2}} + \frac{C_2}{R_{z1}} + \frac{C_{z2}}{R_{Z1}}\right)$$

$$C = \frac{1}{\alpha_2C_1(C_2 + C_{Z2}) + \alpha_2C_{Z1}(C_2 + C_{Z2})}\left(\frac{\alpha_1\alpha_2\beta_{n1}\beta_{P2}}{R_1R_3}\right)$$

$$M = \frac{1}{\alpha_2C_1(C_2 + C_{Z2}) + \alpha_2C_{Z1}(C_2 + C_{Z2})}\left(\frac{\alpha_2C_1}{R_{z2}} + \frac{\alpha_2C_{z1}}{R_{z2}} + \frac{\alpha_2C_2}{R_{z1}} + \frac{\alpha_2C_{Z2}}{R_{Z1}} + \frac{C_4\beta_{P2}}{R_4} + \frac{C_{z1}\beta_{P2}}{R_4}\right)$$

$$N = \frac{1}{\alpha_2C_1(C_2 + C_{Z2}) + \alpha_2C_{Z1}(C_2 + C_{Z2})}\left(\frac{\alpha_1\alpha_2\beta_{n1}\beta_{n2}}{R_2R_3} + \frac{\alpha_2}{R_{Z2}R_{z1}}\right)$$

The non-ideal expressions of IAPF when switch 'S' is closed:

International Journal of Engineering Research & Technology (IJERT)
ISSN: 2278-0181
Vol. 8 Issue 09, September-2019

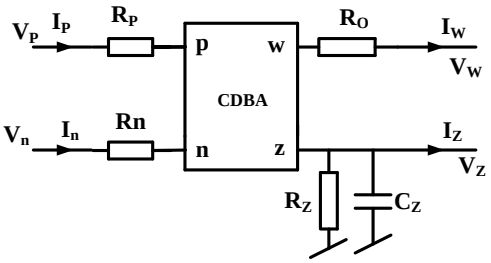

Fig. 3. Non-ideal CDBA with Parasitic elements

$$\left.\frac{V_O(s)}{V_{in}(s)}\right|_{IAPF} = \frac{\frac{1}{\alpha_2}s^2 + Bs + C}{s^2 + Ms + N} \quad (8)$$

where

$$B = \frac{1}{\alpha_2 C_1(C_2 + C_{Z2}) + \alpha_2 C_{Z1}(C_2 + C_{Z2})}\left(\frac{C_1}{R_{z2}} + \frac{C_{Z1}}{R_{z2}} + \frac{C_2}{R_{z1}} + \frac{C_{Z2}}{R_{Z1}} - \frac{\alpha_2\beta_{P2}(C_4 + C_{Z1})}{R_4}\right)$$

$$C = \frac{1}{\alpha_2 C_1(C_2 + C_{Z2}) + \alpha_2 C_{Z1}(C_2 + C_{Z2})}\left(\frac{\alpha_1\alpha_2\beta_{n1}\beta_{P2}}{R_1R_3} - \frac{\alpha_2\beta_{P2}}{R_{z1}R_4}\right)$$

$$M = \frac{1}{\alpha_2 C_1(C_2 + C_{Z2}) + \alpha_2 C_{Z1}(C_2 + C_{Z2})}\left(\frac{\alpha_2 C_4}{R_{z2}} + \frac{\alpha_2 C_{Z1}}{R_{z2}} + \frac{\alpha_2 C_6}{R_{z1}} + \frac{\alpha_2 C_{Z2}}{R_{Z1}} + \frac{C_4\beta_{P2}}{R_4} + \frac{C_{Z1}\beta_{P2}}{R_4}\right)$$

$$N = \frac{1}{\alpha_2 C_1(C_2 + C_{Z2}) + \alpha_2 C_{Z1}(C_2 + C_{Z2})}\left(\frac{\alpha_1\alpha_2\beta_{n1}\beta_{n2}}{R_2R_3} + \frac{\alpha_2}{R_{Z2}R_{z1}}\right)$$

Since the value of R_z is very high and the value of C_z is very low, therefore, the inverse filter transfer functions can be approximated as:

$$\left.\frac{V_0(s)}{V_{in}(s)}\right|_{IBRF} \cong \frac{1}{\frac{s^2}{\alpha_2} + \frac{\alpha_1\beta_{n1}\beta_{P2}}{R_1R_3C_1C_2}}{s^2 + \frac{\beta_{p2}}{C_2R_4}s + \frac{\alpha_1\alpha_2\beta_{n1}\beta_{P2}}{C_1C_2R_2R_3}} \quad (9)$$

which realizes IBRF with cut-off frequency ($\overline{\omega_0}$) and bandwidth ($\overline{BW}$) given by:

$$\overline{\omega_0} = \sqrt{\frac{\alpha_1\alpha_2\beta_{n1}\beta_{n2}}{C_1C_{24}R_2R_3}} = \omega_O\sqrt{\alpha_1\alpha_2\beta_{n1}\beta_{n2}} \quad \text{For } R_1 = R_2$$

$$\overline{BW} = \frac{\beta_{p2}}{C_2R_4} = \beta_{p2}BW \quad (10)$$

and

$$\left.\frac{V_0(s)}{V_{in}(s)}\right|_{IAPF} \cong \frac{1}{\frac{1}{\alpha_2}s^2 - \frac{\beta_{p2}}{\alpha_2C_2R_5}s + \frac{\alpha_1\alpha_2\beta_{n1}\beta_{P2}}{C_2C_4R_1R_3}}{s^2 + \frac{\beta_{p2}}{C_2R_4}s + \frac{\alpha_1\alpha_2\beta_{n1}\beta_{n2}}{C_1C_2R_2R_3}} \quad (11)$$

which realizes IAPF for with $\overline{\omega_0}$, and $\overline{BW}$ given by:

$$\overline{\omega_0} = \sqrt{\frac{\alpha_1\alpha_2\beta_{n1}\beta_{n2}}{C_1C_2(1+\beta_{n_1})R_2R_3}}$$

$$= \omega_O\sqrt{\frac{\alpha_1\alpha_2\beta_{n1}\beta_{n2}}{(1+\beta_{n_1})}} \quad \text{For } R_1 = R_2$$

$$\overline{BW} = \frac{\beta_{p2}}{C_2R_4} = \beta_{P2}BW \quad \text{For } R_5 = R_4 \quad (12)$$

Equations (10) and (12) reveal that the cut-off frequency, and bandwidth of the IBRF and IAPF are dependent on voltage/current tracking error coefficients of the CDBA terminals, hence subsequently introduce errors in the ω_0 and BW of the inverse filters.

IV. SENSITIVITY ANALYSIS

The active and passive sensitivities of ω_0 and *BW* of inverse active filters (IBRF and IAPF) are tabulated in Table 1 which shows that the sensitivities with respect to active and passive components are small.

Table-1 Sensitivity analysis of inverse filters

Filter	Sensitivity
IBRF	$S_{R_2}^{\omega_O} = S_{R3}^{\omega_O} = -\frac{1}{2}, S_{C1}^{\omega_0} = S_{C2}^{\omega_O} = -\frac{1}{2}, S_{R_1}^{\omega_0} = S_{R4}^{\omega_0} = 0$ $S_{\alpha1}^{\omega_O} = S_{\alpha2}^{\omega_0} = S_{\beta_{n2}}^{\omega_O} = \frac{1}{2}, S_{\beta_{p1}}^{\omega_0} = S_{\beta p2}^{\omega_0} = 0$ $S_{R4}^{BW} = S_{C2}^{BW} = -1, S_{R2}^{BW} = S_{R3}^{BW} = S_{C4}^{BW} = 0$ $S_{\beta_{p1}}^{BW} = 0, S_{\beta p2}^{BW} = 1, S_{\alpha1}^{BW} = S_{\alpha2}^{BW} = S_{\beta_{n2}}^{BW} = 0$
IAPF	$S_{R_2}^{\omega_O} = S_{R3}^{\omega_O} = -\frac{1}{2}, S_{C1}^{\omega_0} = S_{C2}^{\omega_O} = -\frac{1}{2},$ $S_{R_1}^{\omega_0} = S_{R_4}^{\omega_0} = S_{R5}^{\omega_O} = 0$ $S_{\alpha1}^{\omega_O} = S_{\alpha2}^{\omega_0} = S_{\beta_{n2}}^{\omega_O} = \frac{1}{2}, S_{\beta_{p1}}^{\omega_0} = S_{\beta p2}^{\omega_0} = 0$

V. SIMULATION RESULTS

The validity of the proposed inverse filters has been examined through PSPICE simulations using an exemplary CMOS CDBA architecture derived from [23], shown here in Fig. 4. The DC power supplies used were ± 2.5V and the bias current was taken 40µA.The aspect ratios used for implementation of CDBA are given in Table 2. The inverse filters were designed for a nominal value of the cut-off frequency of 159 kHz and quality factor Q = 1. The passive components were selected as $C_1 = C_2 = 100$pF, $R_1 = R_2 = R_3$ $R_4 = R_5 = 10$kΩ. Fig. 5 displays the frequency responses of IBRF and Fig. 6 shows the gain and phase responses of IAPF. The tunability of cut-off frequency and quality factor

International Journal of Engineering Research & Technology (IJERT)
ISSN: 2278-0181
Vol. 8 Issue 09, September-2019

of the IBRF have been shown in Fig. 7 and Fig. 8 respectively. The input signal level during PSPICE simulations were kept at 1 V_{PP}.

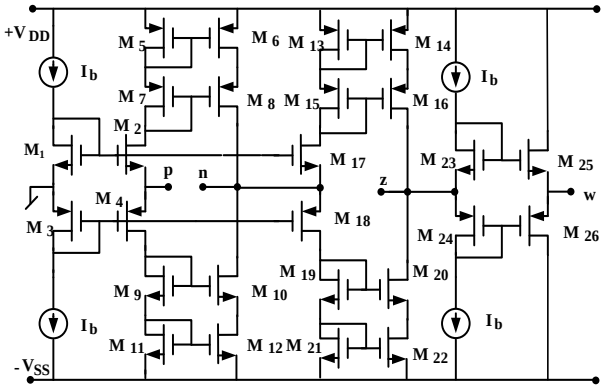

Fig.4 CMOS realization of CDBA derived from [23]

TABLE -2. Aspect ratios of MOSFETs used for realization of CDBA

MOSFETS	$\frac{W}{L}$ratios
M_1,M_2,M_{17},M_{23},M_{25}	50/0.5
M_3,M_4,M_{18},M_{24},M_{26}	100/0.5
M_5-M_{16},M_{19}-M_{22}	3.33/0.5

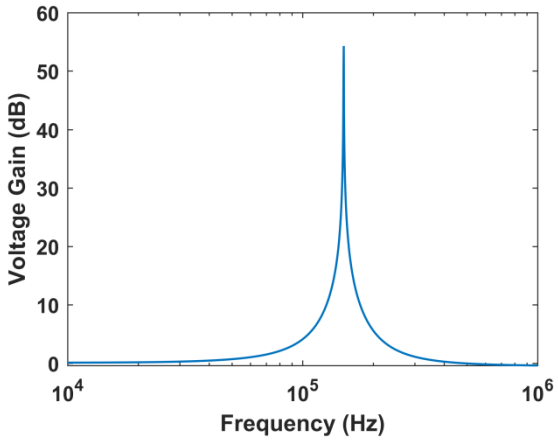

Fig. 5. Frequency responses of IBRF

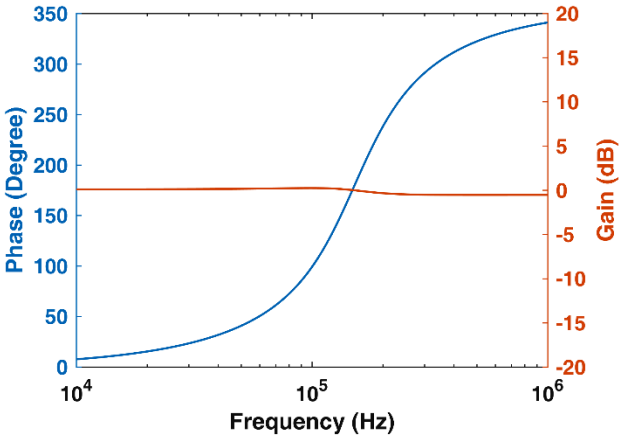

Fig. 6. Gain and phase responses of IAPF

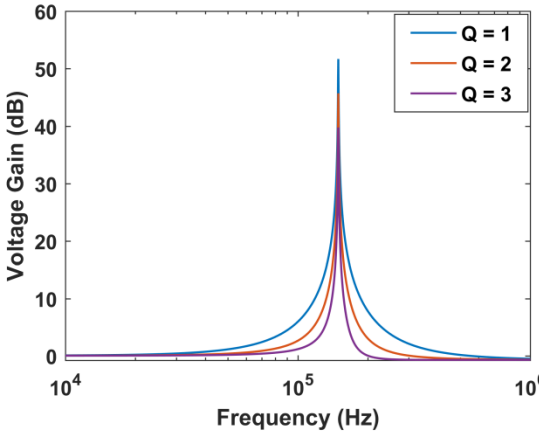

Fig. 7. Tunability of bandwidth for different value of Q for IBRF

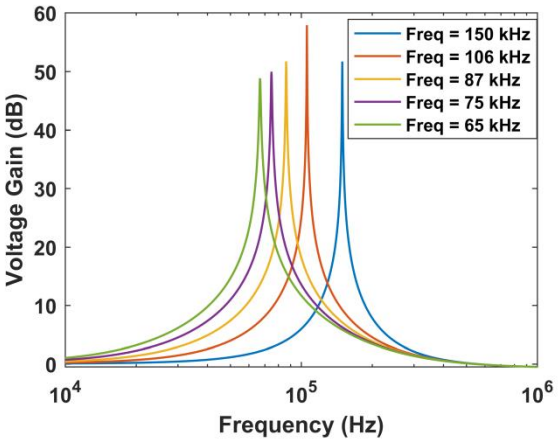

Fig. 8. Tunability of cut-off frequency for IBRF

The Monte Carlo simulation results of the inverse active filters showing variation of gain and cut-off frequency for 5% variation in resistance and capacitance values and have been displayed in Fig. 9 and Fig. 10 respectively. For IBRF the cut-off frequency obtained from the simulations was found to be 150 kHz while Monte Carlo analysis shows that median value of cut-off frequency as 152.148 kHz and similarly for IAPF corresponding to a simulated gain of 0 dB, the Monte Carlo analysis shows that median value of gain as 0.3 dB which shows that the mismatch in the passive component values do not have large effect on the cut-off frequency and gain.

International Journal of Engineering Research & Technology (IJERT)
ISSN: 2278-0181
Vol. 8 Issue 09, September-2019

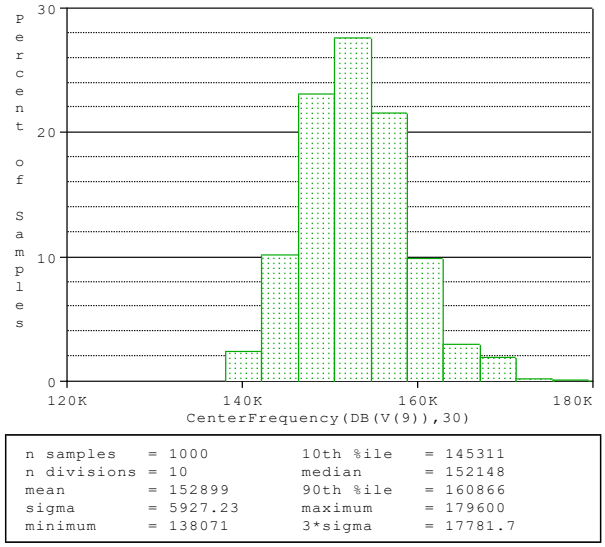

(a)

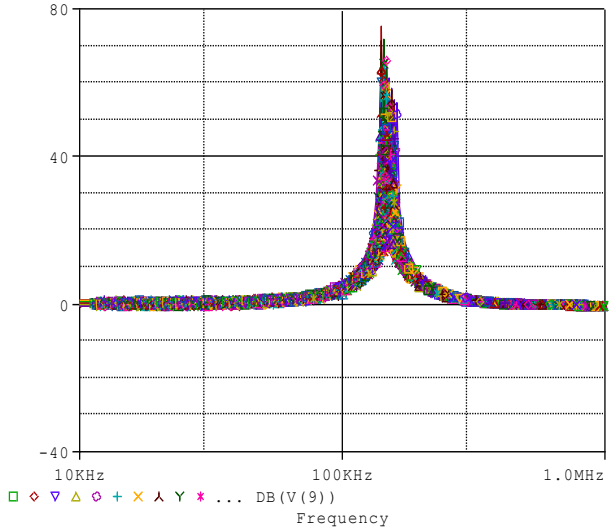

(b)

Fig. 9. Monte-Carlo analysis of IBRF showing variation of cut-off frequency for 5% variation in resistance and capacitance (a) Histogram (b) frequency response.

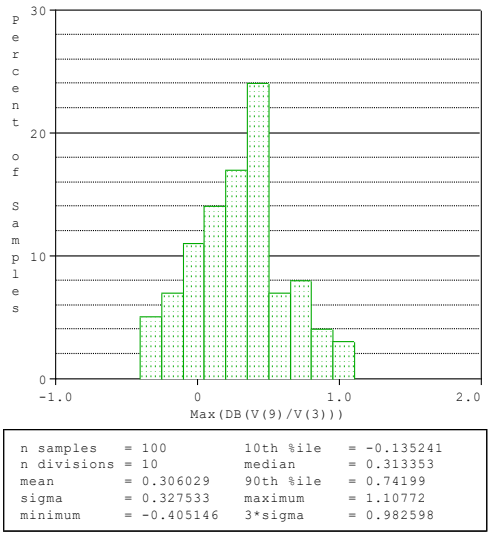

(a)

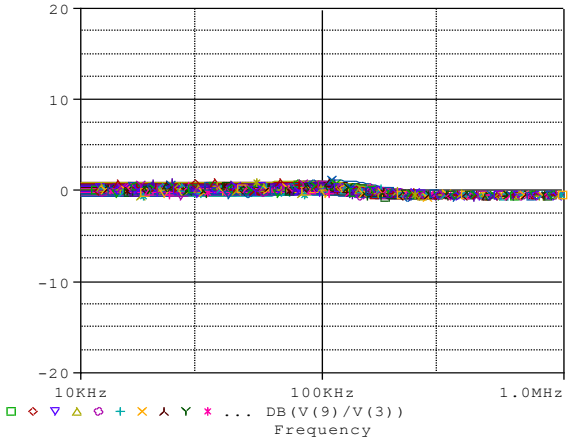

(b)

Fig. 10. Monte-Carlo analysis of IAPF showing variation of gain for 5% variation in resistance and capacitance (a) Histogram (b) frequency response.

VI. CONCLUSIONS

A new VM analog circuit for realizing IBRF and IAPF response has been proposed employing two fully utilised CDBAs, two capacitors, four/five resistors and a switch. The proposed IBRF offers independent tunability of cut-off frequency and quality factor whereas, the IAPF has independent control of cut-off frequency Non-ideal analysis of both the inverse filters has revealed that there is a little error in the cut-off frequency due to inclusion of the parasitic of the CDBAs. The active and passive sensitivities of presented inverse filters are low. The validity of inverse filters has been confirmed through PSPICE simulations using an exemplary CMOS CDBA architecture implemented in TSMC 0.18µm CMOS technology. These simulation results have been found to be in good agreement with the theoretical results.

REFERENCES

[1] Leuciuc, “Using nullors for realization of inverse transfer functions and characteristics”, Electro. Lett., 33(11) (1997), 949–951.
[2] D. R. Bhaskar, M. Kumar, and P. Kumar, “Fractional order inverse filters using operational amplifier”, Analog Integr. Circuits and Signal Process., 97(2018), 149-158.
[3] S. S. Gupta, D. R. Bhaskar, and R. Senani, A.K. Singh, “ Inverse active filters employing CFOA”, Elect. Eng. 1(2009), 23-26.
[4] S. S. Gupta, D.R. Bhaskar, and R. Senani, “New analogue inverse filters realized with current feedback op-amp”, Int. j. of Electro.9(2011),1103–1113.
[5] H. Y. Wang, S.H. Chang, T.Y. Yang, and P.Y. Tsai, “A novel multifunction CFOA based inverse filter”, Circuits and Syst.2(2011),14–17.
[6] K. Garg, R. Bhagat, and B. Jaint, “A novel multifunction modified CFOA based inverse filter”, In Power Electronics (IICPE), IEEE 5th India International Conference. (2012), 1-5.
[7] V. N. Patil, and R. K. Sharma, “Novel inverse active filters employing CFOA”, Int. J. for Scientific Research & Develop. 3(2015), 359–360.
[8] N. A. Shah, and M. F. Rather, “Realization of voltage-mode CCII-based all pass filter and its inversion version”, Indian J. Pure & Applied Physics, 44(2006), 269–271.
[9] T. Tsukutani, Y. Kunugasa, and N. Yabuki, “CCII-Based Inverse Active Filters with Grounded Passive Components”, J. Electr. Eng. 6(2018):212-215.
[10] B. Chipipop, and W. Surakampontorn, “Realization of current-mode FTFN-based inverse filter”, Electron. Lett. 35(1999), 690–692.
[11] H. Y. Wang, and C.T. Lee, “Using nullors for realisation of current-mode FTFN based inverse filters”, Electron. Lett. 35(1999),1889–1890.

International Journal of Engineering Research & Technology (IJERT)
ISSN: 2278-0181
Vol. 8 Issue 09, September-2019

[12] M. T. Abuelma'atti, "Identification of cascadable current-mode filters and inverse-filters using single FTFN", Frequenz , 54(11–12)(2000), 284–289.
[13] A. K. Singh, A. Gupta, and R. Senani, "OTRA-based multi-function inverse filter configuration", Adv. in Elect. and Electron. Eng. 15(2018), 846-856.
[14] A. Pradhan, and R. K. Sharma, "Generation of OTRA-Based Inverse All Pass and Inverse Band Reject Filters", Proceedings of the National Acad. of Sci. India Section A: Physical Sciences, 1-11 (2019)https://doi.org/10.1007/s40010-019-00603-w
[15] A. R. Nasir, and S. N. Ahmad, "A new current mode multifunction inverse filter using CDBA", Int. J. of Comp. Sc. and Info. Security,11(2013),50-52.
[16] R. Pandey, N. Pandey, and T. Negi, V. Garg, "CDBA based universal inverse filter", ISRN Electronics, (2013), 1-6.
[17] A. Sharma, A. Kumar, and P. Whig, "On performance of CDTA based novel analog inverse low pass filter using 0.35 µm CMOS parameter", Int. J. of Sc., Tech. & Manag.4(2015), 594–601.
[18] N. A. Shah, M. Quadri, and S. Z. Iqbal, "High output impedance current-mode all pass inverse filter using CDTA", Indian J. of pure and app. physics,46(2018), 893–896.
[19] T. Tsukutani , Y. Sumi, and N. Yabuki, "Electronically tunable inverse active filters employing OTAs and grounded capacitors", Int. J. of Electron. Lett.4(2016), 166–176.
[20] N. Herencsar , A. Lahiri, J. Koton, and K. Vrba, "Realizations of second-order inverse active filters using minimum passive components and DDCCs", In Proceedings of 33rd Int. Conference on Telecomm. and Signal Proc.-TSP, (2010), 38-41.
[21] P. Kumar, N. Pandey, and S.K. Paul, "Realization of Resistor less and Electronically Tunable Inverse Filters Using VDTA", J. Circuits, Syst. Comp. (2018),1950143.
[22] J.K. Pathak, A. K. Singh, and R. Senani, "Systematic realisation of quadrature oscillators using current differencing buffered amplifiers", IET Circuits, Devices & Syst., 5(2011), 203-211.
[23] A.K. Singh, P. Kumar, "A novel fully differential current mode universal filter", In Circuits and Systems (MWSCAS),2014 IEEE 57th International Midwest Symposium, 579-582(2014).